NANO LETTERS

2008
Vol. 8, No. 12
4653-4658

Electrical Transport and Chemical Sensing Properties of Individual Conducting Polymer Nanowires

Yanyan Cao,[†] Alexey E. Kovalev,[‡] Rui Xiao,[†] Jaekyun Kim,[‡] Theresa S. Mayer,[*,‡] and Thomas E. Mallouk[*,†]

Department of Chemistry, The Pennsylvania State University, University Park, Pennsylvania 16802, Department of Electrical Engineering, The Pennsylvania State University, University Park, Pennsylvania 16802

Received April 3, 2008; Revised Manuscript Received October 22, 2008

ABSTRACT

The electrical transport and chemical sensing properties of individual multisegmented Au-poly(3,4-ethylenedioxythiophene)(PEDOT)-Au nanowires have been investigated. Temperature dependent conductivity measurements show that different charge transport mechanisms influence these properties in two types of PEDOT nanowires. Charge transport in PEDOT/poly(4-styrenesulfonic acid) (PSS) nanowires is in the insulating regime of the metal−insulator transition and dominated by hopping, while PEDOT/perchlorate (ClO_4) nanowires are slightly on the metallic side of the critical regime. The vapor sensing properties of individual nanowires to water and methanol reflect the fact that the two kinds of PEDOT nanowires operate in different transport regimes. Nanowires in the metallic transport regime show much greater sensitivity to vapor-phase analytes than those in which transport is dominated by hopping.

The past decade has witnessed rapid growth in research on conjugated polymer nanostructures, which has been driven by their unique electrochemical and electronic properties, as well as by the processing advantages of polymers relative to inorganic electronic materials. The applications of conducting polymer nanostructures have been recently reviewed.[1] Conducting polymer nanowires and nanotubes have been proposed as active materials for ultrafast electrochromics[2,3] and field emission displays.[4] Nanoresistors, diodes, and field-effect transistors based on conducting polymer nanowires have been demonstrated.[5,6]

Like other high aspect ratio nanostructures such as carbon nanotubes and semiconductor nanowires,[7] conducting polymer nanowires are proming for applications in chemoresistive sensor arrays.[8] Conducting polymer nanowires made by electrochemical replication of porous templates such as anodic aluminum oxide can be grown with precise control over their length and diameter and then integrated into electronic circuits by dielectrophoretic assembly.[9] For chemoresistive sensor applications, it is important to understand the charge transport in nanowires because the charge transport mechansims can have important consequences in terms of the sensor signal-to-noise ratio. Previous studies of poly(3,4-ethylenedioxythiophene) (PEDOT) thin films[10] and nanowires[11] have shown that their electronic behavior is complex and appears to depend on the structure of the polymer, which in turn depends on the synthetic conditions, doping level, charge balancing ions, and other factors, such as the nature of the contacts.

Here, we present data showing that there is a qualitative difference in the charge transport behavior of PEDOT/PSS (PSS = polystyrenesulfonate) and PEDOT/ClO_4 nanowires grown in anodic aluminum oxide templates. Temperature-dependent resistivity measurements show that these nanowires are on the insulating and metallic sides of the metal−insulator (M−I) transition, respectively. Consequently, the two kinds of nanowires exhibit quite different properties in vapor sensing. Possible sensing mechanisms are proposed based on the structural information implied by the transport data.

A typical nanowire in our study consists of three segments: two gold ends and a conducting polymer part in the middle. The nanowires were fabricated by sequential electrodeposition of gold and PEDOT segments in anodic aluminum oxide membranes (see Supporting Information for details). Dark-field optical microscope and transmission electron microscope (TEM) images of the nanowires are shown in Figure 1a. The gold and PEDOT segments can be distinguished clearly in both images because of the high electron density and reflectivity of gold relative to the conducting polymer.

* Corresponding authors. E-mail: tsm2@psu.edu (T.S.M.); tom@chem.psu.edu (T.E.M.).
[†] Department of Chemistry, The Pennsylvania State University.
[‡] Department of Electrical Engineering, The Pennsylvania State University.

10.1021/nl800940e CCC: $40.75
Published on Web 11/01/2008

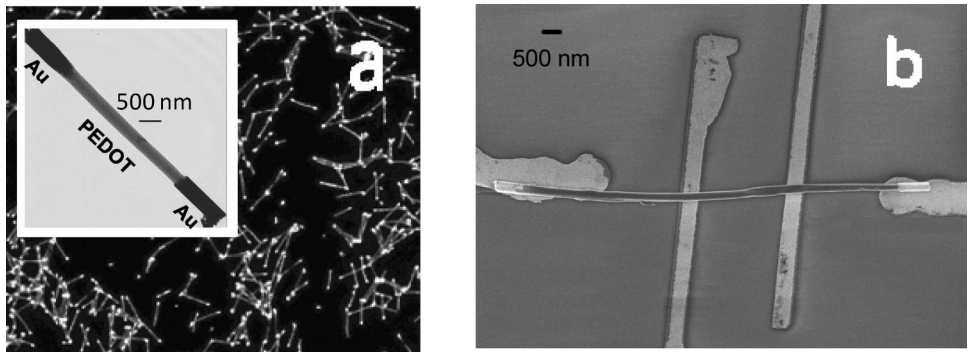

Figure 1. (a) Optical and TEM (inset) images of multisegmented Au-PEDOT/PSS-Au nanowires. (b) Field emission scanning electron microscopy (FE-SEM) image of a Au-PEDOT/PSS-Au nanowire assembled on a four-point measurement test structure.

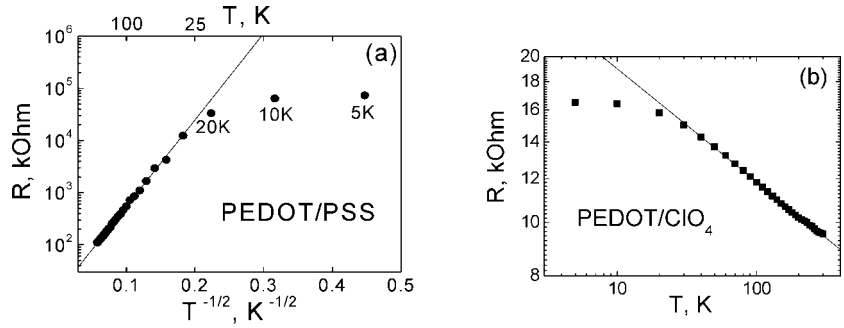

Figure 2. (a) Temperature dependence of the low bias resistance of a PEDOT/PSS nanowire. The straight line is a fit to eq 1. (b) A log−log plot of the temperature dependence of the resistance of a PEDOT/ClO_4 nanowire, which follows a power law at high temperatures (shown by the straight line).

Individual nanowires were aligned in a four-point measurement test bed shown in Figure 1b by dielectrophoretic assembly.[12] The two inner electrodes were fabricated by electron-beam lithography and liftoff of a 10 nm Ti/70 nm Au thick metal electrode deposited by thermal evaporation. Four-point measurements were carried out by monitoring the voltage drop between the two inner electrodes while applying a DC current between the two outer electrodes. A comparison of two-point and four-point resistance showed that the contact resistance between the gold ends and the PEDOT segments was negligible in these nanowires.

The diameters and lengths of the aligned nanowires were estimated from FE-SEM images. The average room temperature conductivity of PEDOT/PSS nanowires was ~5 S/cm, which is slightly lower than the 80 S/cm of electrodeposited PEDOT/PSS films reported in the literature[13,14] possibly due to partial dedoping of the nanowires during the synthesis of the second Au end or subsequent solution processing. The average room temperature conductivity of PEDOT/ClO_4 nanowires was ~200 S/cm.

The temperature dependence of the resistivity has been used extensively to probe the charge transport mechanisms of conducting polymers.[15] Recently, Kaiser reviewed[16] the electrical transport properties in a broad range of conducting polymer films. A fluctuation-induced tunneling model can be used to describe the most highly conducting polymer films, while hopping of charge carriers typically dominates in less conductive films. Hopping transport leads to a rapid increase in resistivity with decreasing temperature. In the critical regime near the metal−insulator (M−-I) transition, the temperature dependence of the resistivity follows a power law. In general, the macroscopic charge transport mechanism is determined by the coexistence and distribution of crystalline domains and disordered regions as well as by the doping level.

The current−voltage (I−V) characteristics of both types of nanowires were measured over the temperature range 5 to 300 K. At temperatures above 30 K, both types of nanowires exhibit ohmic behavior. The temperature dependence of the low bias resistance of the PEDOT/PSS and PEDOT/ClO_4 nanowires is illustrated in parts a and b of Figure 2, respectively. For the PEDOT/PSS nanowires, the resistivity ratio $\rho(20\ \mathrm{K})/\rho(300\ \mathrm{K})$ was ~ 300. The data in the temperature range from 20 to 300 K can be best described by eq 1, as shown in Figure 2a,

$$R(T) \propto \exp[(T_0/T)^{1/2}] \quad (1)$$

where T_0 is between 1000 to 2000 K for different nanowires in this sample. This same temperature dependence and comparable values of T_0 were observed for PEDOT/PSS thin films having conductivities similar to that of our nanowires.[10] The saturation of the resistance at lower temperatures may be explained by the dominant role of tunneling effects in the conductivity when thermal excitation fails to support hopping.

In contrast, the PEDOT/ClO_4 nanowires had a resistivity ratio $\rho(20\ \mathrm{K})/\rho(300\ \mathrm{K}) < 2$. As is shown in Figure 2b, the resistivity in the temperature range from 20 to 300 K follows a power law, which is typically used to describe the critical regime of the M−I transition. A similar temperature depen-

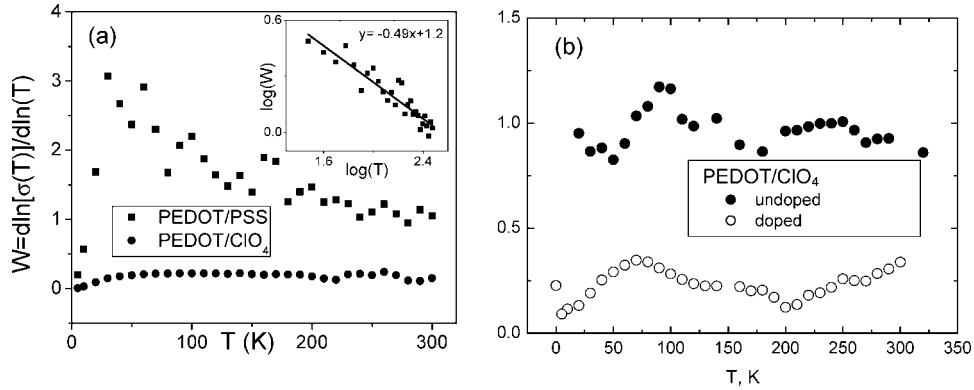

Figure 3. (a) Plot of the reduced activation energy W for PEDOT/PSS and PEDOT/ClO_4 nanowires. (b) Comparison of PEDOT/ClO_4 nanowires before and after electrochemical dedoping.

dence was observed in highly conducting electrochemically deposited PEDOT thin films doped with PF_6, BF_4, and CF_3SO_3.[17]

With crystalline solid state materials, the temperature dependence of the conductivity gives the activation energy, and this method is typically used to differentiate metals from semiconductors and insulators. Metals and insulators have positive and negative values of (d $\ln[\sigma(T)]$)/(d $(1/T)$), respectively. In the case of conducting polymers, the transport properties are dominated by disorder, which results in carrier localization. In this case, the standard method for differentiating insulating, critical, and metallic behavior is to measure the temperature dependence of the reduced activation energy,[15,18] W, which is defined as $W = (\mathrm{d}\ln[\sigma(T)])/(\mathrm{d}\ln T)$. Positive, zero, and negative slopes of the $W-T$ plot correspond to the metallic, critical, and insulating regimes, respectively. As shown in Figure 3a, the PEDOT/PSS nanowire is in the insulating regime with a negative $W-T$ slope over the 30−300 K temperature range. The inset log−log plot Figure 3a shows power law behavior, $W \sim T^{-0.5}$. In contrast, the nearly temperature-independent W of PEDOT/ClO_4 nanowires is characteristic of the critical regime, and its value of around 0.2 indicates that these nanowires are slightly on the metallic side of the M−I transition. To understand if the difference between the PEDOT/PSS and PEDOT/ClO_4 nanowires was simply a consequence of different doping levels, an experiment was done to deliberately dedope the as-prepared PEDOT/ClO_4 nanowires (see Supporting Information for details). The room temperature resistance of the nanowire increases by almost 2 orders of magnitude upon dedoping, and W increases by approximately a factor of 4, but the slope of the $\log(W)-\log(T)$ curve does not change significantly.

The temperature dependence of the resistivity given by eq 1 follows from different models, which all take into account a hopping or variable range hopping (VRH) mechanism. The quasi 1D Mott insulator model[19] assumes that VRH along one direction dominates and T_0 is approximately[20] $B_1/k_BN(E_F)a$, where $N(E_F)$ is the 1D density of states, a is the localization length, and $B_1 > 1$ is a percolation constant. Taking $N(E_F)$ to be about 0.5 eV^{-1} per three-ring PEDOT unit[21] and a to be about the length of the three-ring unit, we obtain $T_0 \geq 23000$ K. This is much higher than the experimentally measured values, and thus it is unlikely that this model can be used to describe charge transport in our PEDOT/PSS nanowires.

Shklovskii and Efros[22] considered 3D VRH with the Coulomb gap at the Fermi level. In this model, the localization length is given by the equation[22] $a = 2.8e^2/k_BT_0\kappa\varepsilon_0$, where e is the electron charge, κ is the dielectric constant, ε_0 is the permittivity of vacuum, and k_B is the Boltzmann constant. Using the experimentally obtained $T_0 = 1000$ K and the typical dielectric constant $\kappa \sim 2$ for conducting polymers, we obtain $a \sim 0.3$ μm, which is physically unreasonable because a typical value of this localization length in conducting polymers does not exceed tens of nanometers.[15] Furthermore, this model is usually applicable at low temperatures in disordered semiconductors, where the transport at higher temperatures is characterized by the 2D or 3D variable range hopping.[23]

There are several other models that predict the temperature dependence of the resistivity in the form of eq 1. For example, the model of Klafter and Sheng[24] for granular conductors takes into account the distribution of grain sizes, while that of Zuppiroli et al.[25] describes hopping between polaronic clusters. Zuppiroli's model assumes variations in dopant distribution. We do not have strong experimental evidence to distinguish between these two models. However, although these two models are based on different microscopic structures, both of them describe hopping between more conducting domains embedded in an insulating matrix.

The charge transport mechanisms that determine the electrical conductivity of the nanowires are determined by the microscopic structure of the conducting polymer, which in turn originates from the synthetic conditions. The difference in the electrical transport properties of PEDOT/PSS and PEDOT/ClO_4 nanowires most likely comes from the different counterions. Similar phenomena were observed in PPy thin films having different counterions.[26] As the size of the counterions increased (from hexafluorophosphate to *p*-toluenesulfonate to sulfonated poly(hydroxyether)), the conductivity decreased and the temperature dependence became stronger. Larger, polymeric counterions are believed not only to increase the spacing between conjugated chain, but also to increase the conformational disorder.[26] As a result, polymers with polyanionic counterions are less crystalline

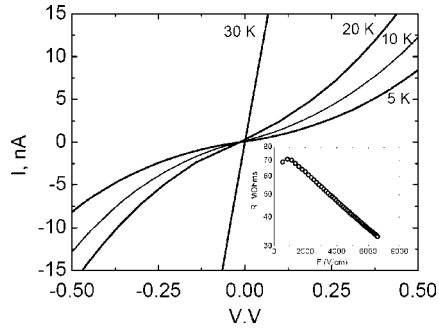

Figure 4. $I-V$ characteristics of a single PEDOT/PSS nanowire measured at three different temperatures. The inset shows the field dependence of the nanowire resistance at 10 K.

than polymers doped with smaller counterions. The perchlorate ion is relatively small ($d \sim 2.8$ Å) and monomeric. Another possible factor is the solvents used in the electrochemical synthesis. Acetonitrile is used in the synthesis of PEDOT/ClO_4, while 1:1 v:v acetonitrile/water is used for PEDOT/PSS synthesis because of the poor solubility of PSS in pure acetonitrile. It is known that aprotic solvents such as acetonitrile improve the integrity of the synthesized polymers because they minimize nucleophilic side reactions[27] that terminate chain propagation.

The temperature-dependent $I-V$ characteristics are symmetric for both types of conducting polymer nanowires. Figure 4 shows $I-V$ plots of a PEDOT/PSS nanowire measured at 30, 20, 10, and 5 K. The nanowires exhibit ohmic behavior at low electric field and/or high temperature. When the temperature decreases below 30 K, the $I-V$ characteristics become nonlinear. In contrast, the PEDOT/ClO_4 nanowires are ohmic over the experimentally measured range of temperatures and fields. Schottky barriers are a common source of nonlinear $I-V$ behavior. However, the influence of metal−polymer contacts on the conduction is eliminated by using the four-point measurement test structure. Thus, it is possible to exclude Schottky emission as the source of the nonlinearity we observed for the PEDOT/PSS nanowires.

From the inset in Figure 4, the logarithm of the nonlinear part of the resistance is proportional to the electric field F inside the sample: $\Delta \ln(R) \sim F$. A similar electric field dependence was obtained by Pollak and Riess[28] for the Mott insulator in the 2D and 3D VRH regime and by Shklovskii and Efros[29] for the 3D VRH regime with a Coulomb gap. Both predicted that the electric field dependence of the resistivity in the intermediate field regime is described as,

$$\ln R = \ln R_0 - \frac{eFL}{k_B T} \tag{2}$$

where R_0 is the low-field resistance, T is the sample temperature, k_B is the Boltzmann constant, and the characteristic length L is on the order of the hopping distance. The hopping distance in these models is temperature dependent and increases as the temperature decreases. On the basis of the discussion above regarding the temperature dependence of the resistivity, it is unlikely that either of these models can explain the nonlinearity observed in PEDOT/PSS nanowires. Nevertheless, eq 2 can be used phenomenologically, where L is considered to be a physically relevant characteristic length. In the region where the temperature dependence of the conductivity follows eq 1, the characteristic length L is nearly temperature independent and is in the range of few nanometers, which is a reasonable distance for hopping in PEDOT/PSS conducting polymers.[30]

Like their macroscopic counterparts, each individual nanowire can function as a chemoresistor to transduce the polymer−analyte interaction into a detectable physical signal. The resistance change of individual nanowires is easily monitored and used as a sensing signal. In general, the nanowires exhibit good reversibility and short response and recovery times upon exposure to water and methanol vapors. Using the definition of 90% of resistance change, the response time and recovery times for PEDOT/PSS are both less than 20 s. For PEDOT/ClO_4 the response and recovery occur within 40 s.

Figure 5 illustrates pronounced differences in the sensing behavior of the two types of nanowires to water and methanol vapors. Both water and methanol vapor induce a decrease in the resistivity of PEDOT/ClO_4 and an increase in the resistivity of the PEDOT/PSS nanowires. We propose different sensing mechanisms for the two types of nanowires. For PEDOT/ClO_4 nanowires, the decrease in resistivity upon solvent vapor exposure possibly results from the partial charge transfer mechanism.[31] Josowicz et al. have proposed this mechanism to explain the sensing behavior of conducting polymers. According to this theory, the difference between the polymer Fermi level E_f and the Mulliken electronegativity E_η, which is defined as the average of its electron affinity and its ionization potential, measures the "driving force" for the weak intermolecular partial charge transfer. The direction of the charge transfer can be inferred from the sensing data. Both water and methanol are acceptors and undergo partial electron transfer from the cationic polymer. Thus, the work function/charge carrier numbers and the conductivity of PEDOT/ClO_4 are increased.

As discussed above, the charge transport in PEDOT/PSS nanowires appears to be dominated by hopping between metallic or highly conducting islands embedded in an insulating matrix. In that case, the simplified model of partial charge transfer is not adequate to explain the interaction between vapors and PEDOT/PSS because the insulating or less conducting regions play an important part in the conduction process. Charlesworth et al. explained their sensing data[32] by modeling the hopping process as an electron-transfer reaction as it occurs in electrochemistry. According to this model, adsorption of solvent vapor increases the resistivity of PPy by decreasing the hopping rate. The resistance of PEDOT/PSS increases upon exposure to solvent vapors because of swelling of the polymer. Swelling increases the hopping distance for charge carriers and thus lowers the conductivity.[33] This mechanism predicts that the resistance should increase upon exposure to almost all volatile organic compounds (VOCs). We observed this behavior with PEDOT/PSS nanowires in response to water, methanol, ethanol, isopropanol, pentanol, acetone, acetonitrile, and dichloromethane.

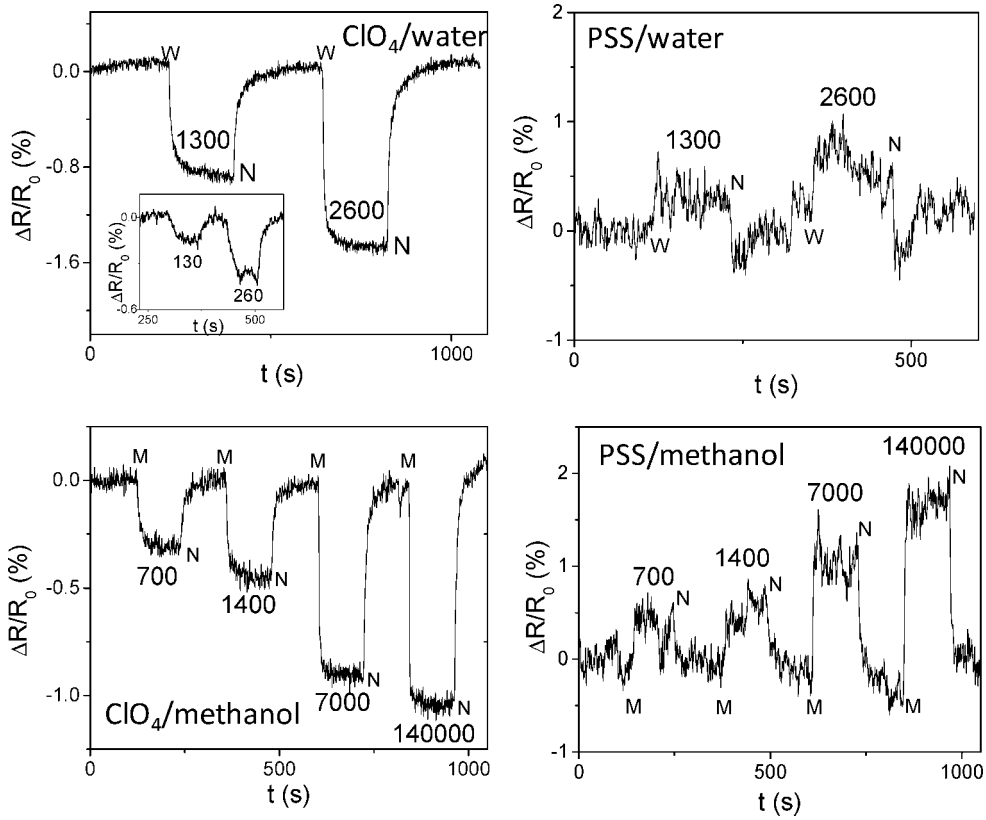

Figure 5. Vapor response of individual PEDOT/ClO_4 and PEDOT/PSS nanowires to water and methanol. The starting point of the vapor flows are marked by "W" (water) and "M" (methanol). "N" indicates the time when nitrogen purging starts. The inset in the top left graph shows the response of a PEDOT/ClO_4 nanowire to low concentrations of water vapor. The vapor concentrations are marked on the graphs in units of parts per million (ppm).

Figure 5 also shows that there is a significant difference in the signal-to-noise ratio between the two kinds of nanowire sensors. PEDOT/ClO_4 offers a much lower baseline noise level than PEDOT/PSS, which leads to better sensitivity and lower detection limit. In fact, a single PEDOT/ClO_4 nanowire can detect water vapor in the range of few tens of ppm, close to the best conducting polymer sensors in the literature.[33,34] The inset in the "ClO_4/water" graph in Figure 5 shows the clear response of a PEDOT/ClO_4 nanowire to 130 ppm and 260 ppm water vapor.

In conclusion, multisegmented Au-PEDOT-Au nanowires synthesized in alumina membranes were assembled into a four-point test structure and characterized individually. The electrical transport properties of the PEDOT/PSS nanowires were found to be on the insulating side of M−-I transition and dominated by a hopping mechanism. In contrast, the PEDOT/ClO_4 nanowires were slightly on the metallic side of the M−I transition. The vapor sensing results of the two types of sensors were compared and different sensing mechanisms were proposed based on the transport data. Water and methanol increased the resistivity of the PEDOT/PSS nanowires and decreased the resistivity of the PEDOT/ClO_4 nanowires. The response of the PEDOT/PSS may be due to an increase of the hopping distance and decrease of the hopping rate in the conducting polymer, while that of the PEDOT/ClO_4 is possibly through partial charge transfer between the polymer and the absorbed vapor molecules.

The logical next step to optimize the sensing performance of PEDOT/ClO_4 nanowires would be (1) to maximize the sensing signal through the adjustment of the polymer doping level or the driving force for partial charge transfer; and (2) to minimize the electrical noise. Under the assumption that the noise is caused by the structural disorder, one can possibly achieve lower noise nanowire sensors through low temperature electrochemical synthesis, which is known[27] to be an effective way to minimize the structural disorder in conjugated polymers.

Acknowledgment. This research was supported by the National Science Foundation under NIRT grant no. ECS-0303981 and the Office of Naval Research through the Counter-IED Program N00014-05-1-0844. We thank Tsung-ta Ho for his assistance in fabricating the four-point measurement test structure. The test structures were fabricated at the PSU Site of the NSF NNIN under agreement no. 0335765.

Supporting Information Available: Experimental methods for nanowire synthesis. Instrumentation for characterization. This material is available free of charge via the Internet at http://pubs.acs.org.

References

(1) (a) Jang, J. In *Emissive Materials: Nanomaterials*; Springer: New York, 2006; Vol. 199, pp 189−259. (b) Groenendaal, L. B.; Jonas, F.; Freitag, D.; Pielartzik, H.; Reynolds, J. R. *Adv. Mater.* **2000**, *12*, 481.
(2) Cho, S. I.; Kwon, W. J.; Choi, S. J.; Kim, P.; Park, S. A.; Kim, J.;

Son, S. J.; Xiao, R.; Kim, S. H.; Lee, S. B. *Adv. Mater.* **2005**, *17*, 171.
(3) Cho, S. I.; Xiao, R.; Lee, S. B. *Nanotechnology* **2007**, *18*, 405705.
(4) Kim, B. H.; Kim, M. S.; Park, K. T.; Lee, J. K.; Park, D. H.; Joo, J.; Yu, S. G.; Lee, S. H. *Appl. Phys. Lett.* **2003**, *83*, 539.
(5) Hurst, S. J.; Payne, E. K.; Qin, L. D.; Mirkin, C. A. *Angew. Chem., Int. Ed.* **2006**, *45*, 2672.
(6) Park, S.; Chung, S. W.; Mirkin, C. A. *J. Am. Chem. Soc.* **2004**, *126*, 11772.
(7) (a) Dai, H. *Acc. Chem. Res.* **2002**, *35*, 1035. (b) Cui, Y.; Wei, Q. Q.; Park, H. K.; Lieber, C. M. *Science* **2001**, *293*, 1289. (c) Xia, Y.; Yang, P.; Sun, Y.; Wu, Y.; Mayers, B.; Gates, B.; Yin, Y.; Kim, F.; Yan, H. *Adv. Mater.* **2003**, *15*, 353.
(8) (a) Zhang, H. Q.; Boussaad, S.; Ly, N.; Tao, N. J. *Appl. Phys. Lett.* **2004**, *84*, 133. (b) Ma, Y.; Zhang, J.; Zhang, G.; He, H. *J. Am. Chem. Soc.* **2004**, *126*, 7097. (c) Ramanathan, K.; Bangar, M. A.; Yun, M.; Chen, W.; Myung, N. V.; Mulchandani, A. *J. Am. Chem. Soc.* **2005**, *127*, 496. (d) Wanekaya, A. K.; Bangar, M. A.; Yun, M.; Chen, W.; Myung, N. V.; Mulchandani, A. *J. Phys. Chem. C* **2007**, *111*, 5218.
(9) (a) Cepak, V. M.; Martin, C. R. *Chem. Mater.* **1999**, *11*, 1363. (b) Hernandez, R. M.; Richter, L.; Semancik, S.; Stranick, S.; Mallouk, T. E. *Chem. Mater.* **2004**, *16*, 3431. (c) Dan, Y.; Cao, Y.; Mallouk, T. E.; Johnson, A. T.; Evoy, S. *Sens. Actuators, B* **2007**, *125*, 55.
(10) Aleshin, A. N.; Williams, S. R.; Heeger, A. J. *Synth. Met.* **1998**, *94*, 173.
(11) Duvail, J. L.; Retho, P.; Garreau, S.; Louarn, G.; Godon, C.; Demoustier-Champagne, S. *Synth. Met.* **2002**, *131*, 123.
(12) Smith, P. A.; Nordquist, C. D.; Jackson, T. N.; Mayer, T. S.; Martin, B. R.; Mbindyo, J.; Mallouk, T. E. *Appl. Phys. Lett.* **2000**, *77*, 1399.
(13) Crispin, X.; Marciniak, S.; Osikowicz, W.; Zotti, G.; Van der Gon, A. W. D.; Louwet, F.; Fahlman, M.; Groenendaal, L.; De Schryver, F.; Salaneck, W. R. *J. Polym. Sci., Part B: Polym. Phys.* **2003**, *41*, 2561.
(14) Zotti, G.; Zecchin, S.; Schiavon, G.; Louwet, F.; Groenendaal, L.; Crispin, X.; Osikowicz, W.; Salaneck, W.; Fahlman, M. *Macromolecules* **2003**, *36*, 3337.
(15) (a) Menon, R.; Yoon, C. O.; Moses, D.; Heeger, A. J. *Handbook of Conducting Polymers*, 2nd ed.; Marcel Dekker Inc.: New York, 1998; pp 27−84. (b) Cho, S.; Heum Park, S.; Heeger, A. J.; Lee, C.-W.; Lee, S.-H. *Nature* **2006**, *441*, 65.
(16) Kaiser, A. B. *Adv. Mater.* **2001**, *13*, 927.
(17) Aleshin, A. N.; Kiebooms, R.; Heeger, A. J. *Synth. Met.* **1999**, *101*, 369.
(18) Zabrodskii, A. G.; Zeninova, K. N. *Sov. Phys. JETP* **1984**, *59*, 425.
(19) Epstein, A. J.; Lee, W. P.; Prigodin, V. N. *Synth. Met.* **2001**, *117*, 9.
(20) Mott, N. F.; Davis, E. A. *Electronic Processes in Non-Crystalline Materials*, 2nd ed.; Clarendon: Oxford, 1979.
(21) Kahol, P. K.; Ho, J. C.; Chen, Y. Y.; Wang, C. R.; Neeleshwar, S.; Tsai, C. B.; Wessling, B. *Synth. Met.* **2005**, *151*, 65.
(22) Efros, A. L.; Shklovskii, B. I. *J. Phys. C* **1975**, *8*, L49.
(23) Rosenbaum, R.; Lien, N. V.; Graham, M. R.; Witcomb, M. *J. Phys.: Condens. Matter* **1997**, *9*, 6247.
(24) Klafter, J.; Sheng, P. *J. Phys. C* **1984**, *17*, L93.
(25) Zuppiroli, L.; Bussac, M. N.; Paschen, S.; Chauvet, O.; Forro, L. *Phys. Rev. B* **1994**, *50*, 5196.
(26) Kohlman, R. S.; Epstein, A. J. *Handbook of Conducting Polymers*. 2nd ed.; Marcel Dekker Inc.: New York, 1998; pp 85−121.
(27) Sadki, S.; Schottland, P.; Brodie, N.; Sabouraud, G. *Chem. Soc. Rev.* **2000**, *29*, 283.
(28) Pollak, M.; Riess, I. *J. Phys. C* **1976**, *9*, 2339.
(29) Shklovskii, B. I.; Efros, A. L. *Electronic Properties of Disordered Semiconductors*; Springer: Berlin, 1984.
(30) Nardes, A. M.; Kemerink, M.; Janssen, R. A. J. *Phys. Rev. B* **2007**, *76*, 085208.
(31) Blackwood, D.; Josowicz, M. *J. Phys. Chem.* **1991**, *95*, 493.
(32) Charlesworth, J. M.; Partridge, A. C.; Garrard, N. *J. Phys. Chem.* **1993**, *97*, 5418.
(33) Bai, H.; Shi, G. Q. *Sensors* **2007**, *7*, 267.
(34) Li, G. F.; Martinez, C.; Semancik, S. *J. Am. Chem. Soc.* **2005**, *127*, 4903.

NL800940E